

Fig. 4. The function $f(D_{el})$ as described in the text is the average of data taken from 20 scans, and is based on 15 different values of D_{el} and 9 reflectivity thresholds (for a total of $9 \times 15 \times 20 = 2700$ dimensions). Averages and standard deviations, indicated by the error bars, are plotted. The least-squares linear regression is shown and has a horizontal intercept ($D_{el} = d_{el}$) of 2.22.

Furthermore, the above formula for $C_{D_{el}}(T_i)$ shows that

$$f(D_{el}) = (D_{el}/d_{el} - 1) \sum_{i=1}^k C_2(T_i) \quad (4)$$

Hence $f(D_{el})$ is linear.

Figure 4 shows the result as D_{el} is varied through 15 values between 3.0 and 2.13; the latter was the lowest value accessible with the data set [this corresponded to boxes of 1 by 1 by 1 pixel and boxes 190 by 190 by 2 pixels (twice the anisotropic scale), where $2.13 = 2 + \log 2/\log 190$]. The same nine thresholds were used as before. The function $f(D_{el})$ was determined separately on 20 radar rain fields; the linear regression shown yields $d_{el} = 2.22 \pm 0.07$. The error is the standard deviation of d_{el} estimated from each of the 20 scans separately. These scans were chosen at random from data from the Montreal region during summer of 1984, all on separate days. The individual slopes and axis intercepts varied by ± 11 and ± 9 percent, respectively, which indicated that any systematic variation is small.

An obvious application of this result is to quantitatively measure the stratification. For example, the rain field is considerably more stratified than the wind field, which has a value $d_{el} = 23/9 = 2.555 \dots$ that has been estimated from energy spectra and dimensional arguments (6). These elliptical dimensions are necessary in both additive (8) and multiplicative [cascade-type (7, 9, 10, 22, 23)] stochastic mesoscale modeling (16). In numerical weather prediction models, the calculated and empirical values of d_{el} can be compared to study the "stochastic coherence" (24) of the calculated values. When fields are stratified, efficient modeling and measurement procedures must involve choosing discrete vertical and horizontal scales that are "comparable"; the elliptical dimension gives us the required exponent. This poses interesting theoretical questions for dynamical models that involve interacting fields with different degrees of stratification.

REFERENCES AND NOTES

1. S. Lovejoy, *Science* **216**, 185 (1982).
2. D. Schertzer and S. Lovejoy, in *Proceedings of the Fourth Symposium on Turbulent Shear Flows* (University of Karlsruhe, West Germany, 1983), p. 11.18.
3. S. Lovejoy and D. Schertzer, in *Preprints, Sixth Symposium on Turbulence and Diffusion* (American Meteorological Society, Boston, 1983), p. 102; D. Schertzer and S. Lovejoy, in *Preprints, Fourth Conference on Atmospheric and Oceanic Waves and Stability* (American Meteorological Society, Boston, 1983), p. 58.
4. D. Schertzer and S. Lovejoy, in *Preprints, International Union of Theoretical and Applied Mechanics Symposium on Turbulence and Chaotic Phenomena in Fluids* (International Union of Theoretical and Applied Mechanics, Kyoto, Japan, 5 to 10 September 1983) p. 141.
5. ———, *Turbulence and Chaotic Phenomena in Fluids*, T. Tatsumi, Ed. (North-Holland, Amsterdam, 1984), p. 505.
6. ———, in *Turbulent Shear Flow*, L. J. Bradbury and F. Durst, Eds. (Springer, New York, 1985), vol. 4, pp. 7–33.
7. ———, *Phys. Chem. Hydrodyn.* **6**, 623 (1985).
8. S. Lovejoy and D. Schertzer, *Water Resour. Res.* **21**, 1233 (1985).
9. D. Schertzer and S. Lovejoy, *Fractals in Physics*, S. Pietronero and E. Tosatti, Eds. (North-Holland, Amsterdam, 1986), p. 457.
10. ———, *J. Geophys. Res.*, in press.
11. H. G. E. Hentschel and I. Procaccia, *Physica* **8D**, 435 (1983).
12. P. Grassberger, *Phys. Lett.* **97A**, 227 (1983).
13. U. Frisch and G. Parisi, in *Turbulence and Predictability in Geophysical Fluid Dynamics and Climate Dynamics*, M. Ghil, R. Benzi, G. Parisi, Eds. (North-Holland, Amsterdam, 1985), p. 84.
14. T. C. Halsey, M. H. Jensen, L. P. Kadanoff, I. Procaccia, B. I. Shraiman, *Phys. Rev. A* **33**, 1141 (1986).
15. S. Lovejoy and D. Schertzer, *Digital Image Processing in Remote Sensing*, J. P. Muller, Ed. (Francis and Taylor, London, in press), chap. 14.
16. ———, *Bull. Am. Meteorol. Soc.* **67**, 21 (1986).
17. ———, P. Ladoy, *Nature (London)* **319**, 43 (1986).
18. ———, *ibid.* **320**, 401 (1986).
19. P. Gabriel, S. Lovejoy, G. L. Austin, D. Schertzer, in *Preprints, Sixth Conference on Atmospheric Radiation* (American Meteorological Society, Boston, 1986), p. 230.
20. The standard error of the fits was computed. The maximum value for all the fits (the largest T was used) was ± 0.07 .
21. B. Kerman, K. Szeto, S. Lovejoy, D. Schertzer, in *Preprints, Nonlinear Variability in Geophysics* (McGill University, Montreal, 1986), p. 34.
22. D. Schertzer and S. Lovejoy, *Ann. Math. Quebec* in press.
23. Multiplicative processes are required if we are to obtain the necessary hierarchy of fractal dimensions.
24. D. Schertzer et al., in *Preprints, International Association of Meteorology and Atmospheric Physics and the World Meteorological Organization Symposium on the Maintenance of the Quasi-Stationary Components of the Flow in the Atmosphere and in Atmospheric Models*, (World Meteorological Organization, Geneva, 1983), p. 325.
25. We acknowledge discussions with G. L. Austin, P. Gabriel, V. K. Gupta, J. P. Kahane, P. Ladoy, D. Lavallée, E. Levitch, J. P. Muller, R. Peschanski, A. Saucier, T. Warn, E. Waymire, and J. Wilson. We thank the Aspen Center for Physics for their hospitality.

23 September 1986; accepted 6 January 1987

Foam Structures with a Negative Poisson's Ratio

RODERIC LAKES

A novel foam structure is presented, which exhibits a negative Poisson's ratio. Such a material expands laterally when stretched, in contrast to ordinary materials.

VIRTUALLY ALL COMMON MATERIALS undergo a transverse contraction when stretched in one direction and a transverse expansion when compressed. The magnitude of this transverse deformation is governed by a material property known as Poisson's ratio. Poisson's ratio is defined as the negative transverse strain divided by the axial strain in the direction of stretching force. Since ordinary materials contract laterally when stretched and expand laterally when compressed, Poisson's ratio for such materials is positive. Poisson's ratios for various materials are approximately 0.5 for rubbers and soft biological tissues, 0.45 for lead, 0.33 for aluminum, 0.27 for common steels, 0.1 to 0.4 for typical polymer foams, and nearly zero for cork.

Negative Poisson's ratios are theoretically permissible but have not, with few exceptions, been observed in real materials. Specifically, in an isotropic material (a material that does not have a preferred orientation) the allowable range of Poisson's ratio is from -1.0 to $+0.5$, based on thermodynamic considerations of strain energy in the

theory of elasticity (1). It is believed by many that materials with negative values of Poisson's ratio are unknown (1); however, Love (2) presented a single example of cubic "single crystal" pyrite with a Poisson's ratio of -0.14 and he suggested that the effect may result from a twinned crystal. Analysis of the tensorial elastic constants of anisotropic single crystal cadmium suggests that Poisson's ratio may attain negative values in some directions (3). Anisotropic, macroscopic two-dimensional flexible models of certain honeycomb structures (not materials) have exhibited negative Poisson's ratios in some directions (4). These known examples of negative Poisson's ratios all depend on the presence of a high degree of anisotropy; the effect only occurs in some directions and may be dominated by coupling between stretching force and shear deformation. The materials described in this report, by contrast, need not be anisotropic.

Foams with negative Poisson's ratios were

University of Wisconsin, Madison

produced from conventional low-density open-cell polymer foams (Fig. 1) by causing the ribs of each cell to permanently protrude inward; this resulted in a reentrant structure such as that shown in Fig. 2. An idealized reentrant unit cell is shown in Fig. 3. A polyester foam (5) was used as a starting material and was found to have a density of 0.03 g cm^{-3} , a Young's modulus of 71 kPa, a cell size of 1.2 mm, and a Poisson's ratio of 0.4. The method used to create the reentrant structure is as follows. Specimens of conventional foam were compressed triaxially, that is, in three orthogonal directions, and were placed in a mold. The mold was heated to a temperature slightly above the softening temperature of the foam material, 163° to 171°C in this case. The mold was then

cooled to room temperature and the foam was extracted. Specimens that were given a permanent volumetric compression factor of between 1.4 and 4 during this transformation were found to exhibit negative Poisson's ratios. For example, a foam subjected to a permanent volumetric compression factor of 2 had a Young's modulus of 72 kPa, and a Poisson's ratio of -0.7 . Polyester foams of similar structure and properties, but different cell sizes (0.3, 0.4, and 2.5 mm), transformed by the above procedure were also found to exhibit negative Poisson's ratios. Reticulated metal foams were transformed by the alternate procedure of plastically deforming the material at room temperature. Permanent compressions were performed sequentially in each of three or-

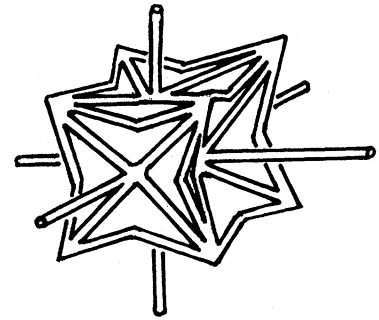


Fig. 3. Idealized reentrant unit cell produced by symmetrical collapse of a 24-sided polyhedron with cubic symmetry.

thogonal directions. Foams transformed in this way were also found to exhibit reentrant structures.

The casual observer may comment that materials with negative Poisson's ratios are counterintuitive in that they do not conserve volume. This is not objectionable since there is no law of conservation of volume. Various observers develop insights about these physical properties from rubbery materials that are indeed nearly incompressible. Nevertheless, such common materials such as steel, aluminum, conventional foams, and hard plastics have Poisson's ratios that differ from 0.5, hence these materials do not conserve volume. All known materials, including the ones described here, obey conservation of energy, which restricts Poisson's ratio to be between -1.0 and 0.5 for isotropic materials. The physical origin of the negative Poisson's ratio can be appreciated in view of the idealized unit cell shown in Fig. 3. Tension applied to the vertical links will cause the cell to unfold and expand laterally. The actual cell structure (Fig. 2) also contains ribs which are bent and protrude into the cells.

Foams with negative Poisson's ratios were found to be more resilient than conventional foams. Foams with a typical structure of tetrakaidecahedral (14-sided) cells (6) exhibit an approximately linear compressive stress-strain curve up to about 5% strain (7). At higher strains, the cell ribs buckle and the foam collapses at constant stress. Reentrant foams exhibited a nearly linear relation between stress and strain up to more than 40% strain, with no abrupt collapse. Resilience was enhanced for deformation in each of three orthogonal directions. Improved resilience (in one direction) has also been reported in foams compressed permanently in one direction (uniaxially) (8). I prepared such foams and found that they exhibited Poisson's ratios near zero. They did not exhibit negative values.

It is notable that the theory of elasticity contains no characteristic length scale. The

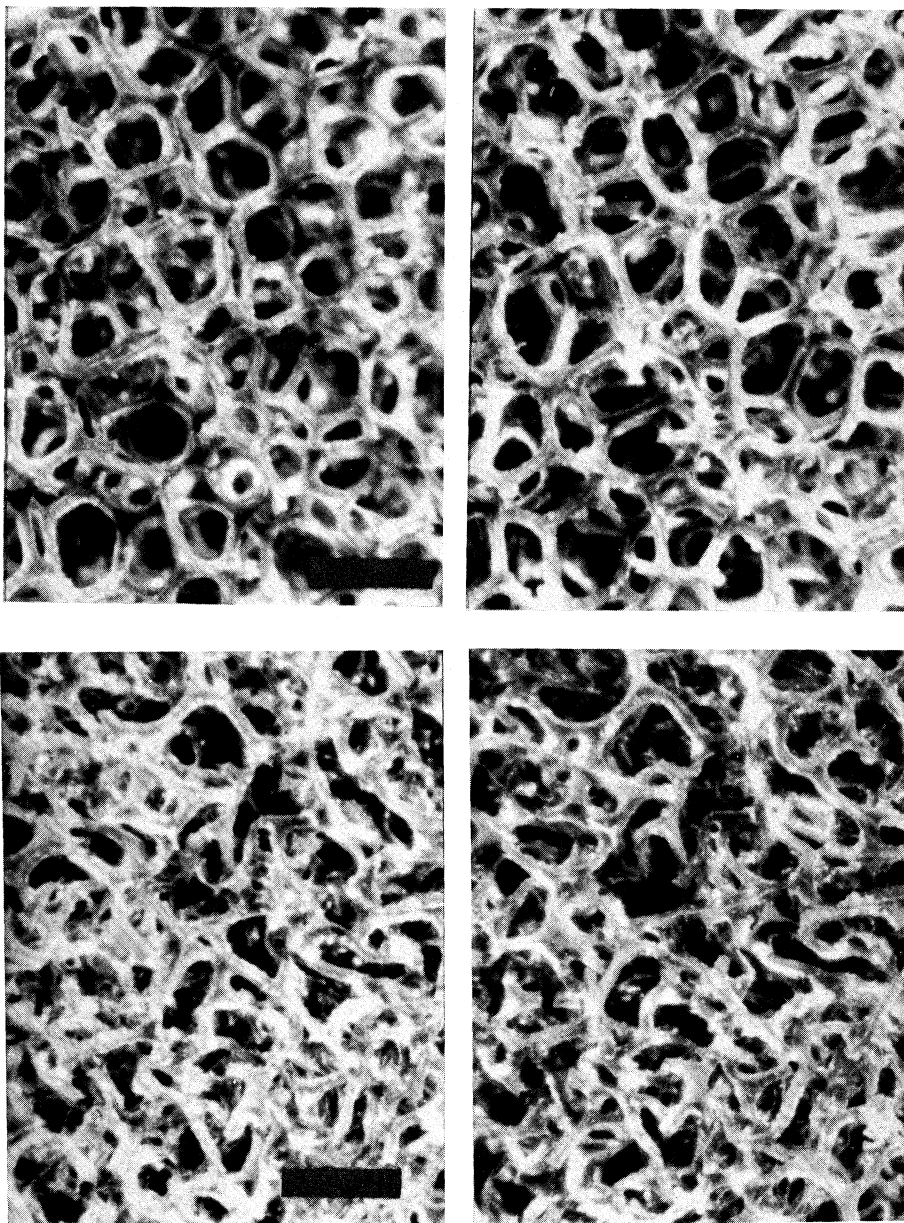


Fig. 1 (top). Stereo photograph of a conventional open-cell polymer foam. Scale mark, 2 mm. **Fig. 2 (bottom).** Stereo photograph of a reentrant foam. Permanent volumetric compression factor is 2.7. Poisson's ratio is -0.6 . Scale mark, 2 mm.

phenomenon of a negative Poisson's ratio consequently does not require a coarse cellular structure or depend on the structure size. In principle, materials with microstructure on a scale smaller than 1 μm could exhibit a negative Poisson's ratio. The theory of elasticity also predicts a variety of unusual phenomena to occur in solids with a negative Poisson's ratio. For example, the top and bottom lateral surfaces of a bent prismatic beam of a conventional material with a positive Poisson's ratio assume a saddle shape: the "anticlastic curvature" of bending, in which the transverse curvature is opposite the principal curvature of bending (9). In the case of a negative Poisson's ratio, the theory of elasticity predicts that these surfaces will assume an ellipsoidal shape, or a synclastic curvature. I have observed such synclastic curvature in bent bars of transformed foam. Furthermore, in the indentation of a block of material caused by a localized pressure distribution, the indentation for a given pressure is proportional to $(1 - \nu^2)/E$, in which E is Young's modulus and ν is Poisson's ratio. Consequently, a material with a negative Poisson's ratio approaching the thermodynamic limit $\nu = -1.0$ will be difficult to indent even if the material is compliant. The origin of this predicted phenomenon may be traced to the relation between the shear modulus G , the bulk modulus B (the inverse of the compressibility), and Poisson's ratio ν : $B = 2G(1 + \nu)/(1 - 2\nu)$. When the Poisson's ratio approaches 0.5, as in rubbery solids, the bulk modulus greatly exceeds the shear modulus and the material is referred to as incompressible. When Poisson's ratio approaches -1.0 , the material becomes highly compressible; its bulk modulus is much less than its shear modulus. The toughness of a material can also depend on its Poisson's ratio. Specifically, the critical tensile stress (10) for fracture of a solid of surface tension T , Young's modulus E , with a plane circular crack of radius r is $[\pi ET/2r(1 - \nu^2)]^{1/2}$. When the Poisson's ratio approaches -1.0 , the material is predicted to become very tough.

Applications of novel, reentrant foams with negative Poisson's ratios may be envisaged in view of these properties. An example of the practical application of a particular value of Poisson's ratio is the cork of a wine bottle. The cork must be easily inserted and removed, yet it also must withstand the pressure from within the bottle. Rubber, with a Poisson's ratio of 0.5, could not be used for this purpose because it would expand when compressed into the neck of the bottle and would jam. Cork, by contrast, with a Poisson's ratio of nearly zero, is ideal in this application. It is anticipated that

reentrant foams may be used in such applications as sponges, robust shock-absorbing material, air filters, and fasteners.

REFERENCES AND NOTES

1. Y. C. Fung, *Foundations of Solid Mechanics* (Prentice-Hall, Englewood Cliffs, NJ, 1968), p. 353.
2. A. E. H. Love, *A Treatise on the Mathematical Theory of Elasticity* (Dover, New York, ed. 4, 1944).
3. Y. Li, *Phys. Status Solidi* **38**, 171 (1976).
4. L. J. Gibson, M. F. Ashby, G. S. Schajer, C. I. Robertson, *Proc. R. Soc. London A* **382**, 25 (1982).
5. Scott Industrial Foam, Scott Paper Company.
6. H. A. Lanceley, J. Mann, G. Pogany, in *Composite Materials*, L. Holliday, Ed. (Elsevier, New York, 1966), chap. 6.
7. M. F. Ashby, *Metall. Trans.* **14A**, 1755 (1983).
8. W. R. Powers, U.S. Patent 3 025 200 (1962).
9. S. P. Timoshenko and J. N. Goodier, *Theory of Elasticity* (McGraw-Hill, New York, ed. 3, 1982).
10. I. N. Sneddon, *Fourier Transforms* (McGraw-Hill, New York, 1951).
11. I thank the University of Iowa Research Foundation for filing a patent application for this invention. Specimens of polyester foam were kindly supplied by Foamade Industries, Auburn Hills, MI.

6 October 1986; accepted 6 January 1987

Encystation and Expression of Cyst Antigens by *Giardia lamblia* in Vitro

FRANCES D. GILLIN, DAVID S. REINER, MICHAEL J. GAULT, HERNDON DOUGLAS, SIDDHARTHA DAS, ANNETTE WUNDERLICH, JUDITH F. SAUCH

The cyst form of *Giardia lamblia* is responsible for transmission of giardiasis, a common waterborne intestinal disease. In these studies, encystation of *Giardia lamblia* in vitro was demonstrated by morphologic, immunologic, and biochemical criteria. In the suckling mouse model, the jejunum was shown to be a major site of encystation of the parasite. Small intestinal factors were therefore tested as stimuli of encystation. An antiserum that reacted with cysts, but not with cultured trophozoites was raised in rabbits and used as a sensitive probe for differentiation in vitro. Cultured trophozoites that were exposed to bile salts showed a more than 20-fold increase in the number of oval, refractile cells that reacted strongly with anticyst antibodies, and in the expression of major cyst antigens. Exposure to primary bile salts resulted in higher levels of encystation than exposure to secondary bile salts. These studies will aid in understanding the differentiation of an important protozoan pathogen.

GIARDIASIS, A MAJOR HUMAN INTESTINAL disease worldwide, is transmitted by ingestion of the oval cyst form of *Giardia lamblia* from fecally contaminated water or food (1). Exposure of cysts to gastric acid triggers excystation in the duodenum (2). Emerging flagellated trophozoites divide and colonize the small intestine where some remain and cause diarrhea, while others encyst and are passed in feces, completing the life cycle (3). Although trophozoites can be cultured in vitro (4), neither encystation nor expression of cyst antigens in vitro has been reported. The studies presented here were designed to (i) elucidate the process of encystation in vivo; (ii) develop sensitive reagents for the detection and quantitation of differentiation in vitro; and (iii) develop a system for induction of encystation of trophozoites cultured in vitro.

Since little is known about encystation of *G. lamblia*, we studied the location of cysts and trophozoites along the small and large intestine of suckling mice as a function of time after infection. Three-day-old suckling mice (strain CF1) were infected (5) with 10^3 axenically cultured *G. lamblia* trophozoites

by direct transcutaneous injection into the milk-filled stomach (6). Trophozoites of strain WB (ATCC #30957) had been grown to late log phase in supplemented (6) Diamond's TYI-S-33 medium (7) as described (8), washed, and resuspended in 0.2 ml of 0.1M phosphate-buffered saline (PBS; pH 7.2). We found cysts in every intestinal section, although few were in the duodenal section "D" (Fig. 1). Through day 16, large numbers of cysts were in sections 3 or 4 (mid to lower jejunum). As infection progressed, increasing proportions of cysts were found in the large intestine. Since cysts are not motile and therefore move downstream with the flow of intestinal fluid, sections 3 and 4 appeared to be major sites of encystation. The percentage of parasites in cyst form per mouse averaged 8.6 (from nine determinations, days 4 through 20, range,

F. D. Gillin, D. S. Reiner, M. J. Gault, S. Das, Department of Pathology, University of California, San Diego Medical Center H811F, San Diego, CA 92103. A. Wunderlich and H. Douglas, Department of Medicine, University of California, San Diego Medical Center H811F, San Diego, CA 92103. J. F. Sauch, Health Effects Research Laboratory, U.S. Environmental Protection Agency, Cincinnati, OH 45268.